

Acid-Promoted Homogeneous Hydrogenation of Alkenes Catalyzed by the Ruthenium–Hydride Complex (PCy₃)₂(CO)(Cl)RuH: Evidence for the Formation of 14-Electron Species from the Selective Entrapment of the Phosphine Ligand

Chae S. Yi,* Do W. Lee, and Zhengjie He

Department of Chemistry, Marquette University, Milwaukee, Wisconsin 53201-1881

Arnold L. Rheingold, Kin-Chung Lam, and Thomas E. Concolino

Department of Chemistry, University of Delaware, Newark, Delaware 19716

Received April 13, 2000

The addition of 1.0 equiv of HBF₄·OEt₂ led to a ca. 2–3-fold increase in the catalyst activity of (PCy₃)₂(CO)(Cl)RuH (**1a**) toward the hydrogenation of alkenes. The stoichiometric reaction of **1a** with HBF₄·OEt₂ produced a 1:3.5 mixture of the new ruthenium–hydride species **2** and Cy₃PH⁺BF₄[−]. The catalyst activity of the isolated **2**/Cy₃PH⁺ mixture was found to be similar to **1a**/HBF₄·OEt₂. The complex **2** slowly decomposed in C₆H₆ solution to give a novel tetrameric complex **3**. The treatment of **1a** with HBF₄·OEt₂ in CH₃CN led to the selective formation of the monophosphine species **4**, which was converted to the stable complex **5** upon treatment with excess PPh₃. The reaction of **1a** with a weak acid, HSiCl₃, led to the formation of the anionic silyl complex **7**. The structures of **3**, **5**, and **7** were determined by X-ray crystallography. The formation of η²-H₂ complex **8** was observed by NMR at low temperature. These results suggested that the 14-electron species [(PCy₃)₂(CO)RuHCl], generated from the selective entrapment of the phosphine ligand, is the key species involved in the catalytic hydrogenation reaction.

Introduction

The dissociation of a phosphine ligand is one of the most common ways to activate metal–phosphine complexes.¹ For example, metal–phosphine complexes such as (PPh₃)₃RhCl (hydrogenation),² (PPh₃)₃(CO)RhH (hydroformylation),³ and (PCy₃)₂(Cl)₂Ru=CHPh (metathesis)⁴ have been well-known to generate catalytically active species via an initial dissociation of the phosphine ligand. As a way to increase the catalyst activity, considerable efforts have been directed to develop methods for selectively promoting the dissociation and trapping of phosphine ligands. Grubbs and co-workers observed a substantial rate enhancement of the metathesis catalytic activity of (PCy₃)₂(Cl)₂Ru=CHPh upon

addition of CuCl to the reaction mixture.^{4b} The formation of an adduct PCy₃·CuCl has been suggested for generating a highly reactive 14-electron monophosphine ruthenium–alkylidene complex. Also reported was up to a 10-fold rate increase in the catalyst activity when HCl was added to a water-soluble analogue of the ruthenium–alkylidene complex.⁵ Using BPh₃ as a Lewis acid, Berry and co-workers recently demonstrated an effective entrapment of PMe₃ ligand in forming a novel ruthenium–silene complex (PMe₃)₃Ru(η²-CH₂=SiMe₃)-H₂.⁶ Lewis acids have also been well-known to promote the hydrogenation of unsaturated compounds.^{7–9} Some of the representative examples include the transfer hydrogenation of aryl-substituted olefins by Pd/C and AlCl₃⁸ and the hydrogenation of aromatic compounds by Ni(acac)₂/AlEt₃.⁹

While studying the ruthenium-catalyzed hydrovinyl-ation reactions of alkynes, we recently observed the formation of the phosphonium salt Cy₃PH⁺BF₄[−] in the reactions catalyzed by the cationic ruthenium complex [(PCy₃)₂(CO)(Cl)Ru=CHCH=C(CH₃)₂]⁺BF₄[−].¹⁰ The for-

(1) (a) Collman, J. P.; Hegedus, L. S.; Norton, J. R.; Finke, R. G. *Principles and Applications of Organotransition Metal Chemistry*; University Science Books: Mill Valley, CA, 1987. (b) *Homogeneous Catalysis with Metal Phosphine Complexes*; Pignolet, L. H., Ed.; Plenum Press: New York, 1983.

(2) (a) Chaloner, P. A.; Esteruelas, M. A.; Joó, F.; Oro, L. A. *Homogeneous Hydrogenation*; Kluwer: Boston, 1994. (b) Brunner, H. In *Applied Homogeneous Catalysis with Organometallic Compounds*; Cornils, B., Herrmann, W. A., Eds.; VCH: New York, 1996; Vol. 1.

(3) (a) Parshall, G. W.; Ittel, S. D. *Homogeneous Catalysis*, 2nd ed.; Wiley & Sons: New York, 1992. (b) Frohning, C. D.; Kohlpaintner, C. W. In *Applied Homogeneous Catalysis with Organometallic Compounds*; Cornils, B., Herrmann, W. A., Eds.; VCH: New York, 1996; Vol. 1.

(4) (a) Nguyen, S. T.; Grubbs, R. H.; Ziller, J. W. *J. Am. Chem. Soc.* **1993**, *115*, 9858–9859. (b) Dias, E. L.; Nguyen, S. T.; Grubbs, R. H. *J. Am. Chem. Soc.* **1997**, *119*, 3887–3897. (c) Dias, E. L.; Grubbs, R. H. *Organometallics* **1998**, *17*, 2758–2767. (d) Ulman, M.; Grubbs, R. H. *Organometallics* **1998**, *17*, 2484–2489.

(5) Lynn, D. M.; Mohr, B.; Grubbs, R. H. *J. Am. Chem. Soc.* **1998**, *120*, 1627–1628.

(6) Dioumaev, V. K.; Plössl, K.; Caroll, P. J.; Berry, D. H. *J. Am. Chem. Soc.* **1999**, *121*, 8391–8392.

(7) Olah, G. A.; Molnár, A. *Hydrocarbon Chemistry*; Wiley: New York, 1995.

(8) Olah, G. A.; Prakash, G. K. S. *Synthesis* **1978**, 397–398.

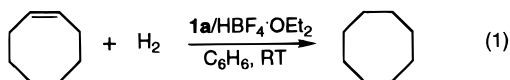
(9) (a) Lapporte, S. J.; Schuett, W. R. *J. Org. Chem.* **1963**, *28*, 1947–1948. (b) Sloan, M. F.; Matlack, A. S.; Breslow, D. S. *J. Am. Chem. Soc.* **1963**, *85*, 4014–4019.

Table 1. Effect of Addition of Acids on the Hydrogenation of Cyclooctene Catalyzed by 1^a

entry	catalyst	acid	turnover rate ^b
1	1a	none	940
2	1b	none	760
3	1a	HBF ₄ ·OEt ₂	2200
4	1b	HBF ₄ ·OEt ₂	600
5	1a	HOTf	2200
6	1a	CF ₃ CO ₂ H	310
7	1a	HCl·OEt ₂	~0 ^c
8	1a	CuCl ₂	700
9	1a	BBh ₃	1080
10	1a	PdCl ₂	150

^a Reaction conditions: 5.7 mmol of alkene (1.0 M); 0.69 μmol of the catalyst (0.12 mM; alkene:1 = 8300:1); 0.7–1.4 μmol of acid; 1.0 atm H₂; 5 mL of C₆H₆; 22 ± 1 °C. ^b Turnover rate = (mol of product)/(mol of catalyst) h⁻¹. ^c The catalyst decomposed upon the addition of acid.

mation of Cy₃PH⁺BF₄⁻ appeared to promote the catalytic activity of the ruthenium complex. These results suggested that the phosphonium salt formation may be a viable way for sequestering dissociated phosphine ligands. Herein we wish to report an acid-induced selective entrapment of the phosphine ligand on the ruthenium–hydride complex (PCy₃)₂(CO)(Cl)RuH (**1a**). We also present evidence of the formation of a mono-phosphine intermediate species and its role in the catalytic hydrogenation of alkenes.



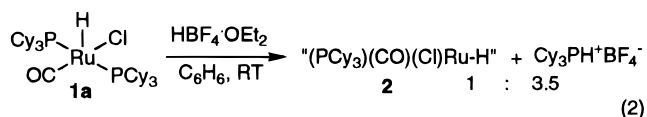
Results and Discussion

Effect of Acids on the Rate of Hydrogenation of Alkenes. We recently reported that the ruthenium–hydride complex **1a** is an effective catalyst for the hydrogenation of alkenes and proposed the mechanism of reaction via an initial dissociation of the phosphine ligand.¹¹ In an effort to increase the catalyst activity, we explored the effect of adding acids on the catalyst activity toward the hydrogenation reaction of cyclooctene (eq 1). Among the selected group of acids, the most significant rate enhancement was observed with protic acids with weakly coordinating anions, HOTf and HBF₄·OEt₂ (Table 1). For example, the treatment of cyclooctene with 1.0 atm of H₂ in the presence of **1a** and 1.0 equiv of HBF₄·OEt₂ at room temperature resulted in a turnover rate of 2200 h⁻¹, which was more than 2 times higher than the reaction catalyzed by **1a** under similar reaction conditions (entry 3). In contrast, the addition of HBF₄·OEt₂ to the PPr₃ analogue (PPr₃)₂(CO)(Cl)RuH (**1b**) did not lead to a rate increase compared to **1b** alone (entry 4).¹² Only a marginal increase in catalyst activity was observed with Lewis acids, CuCl₂ and BPh₃ (entries 8, 9), while a decrease in catalyst activity was observed for protic acids with

coordinating anions such as CF₃CO₂H and HCl·OEt₂ (entries 6, 7).

We next surveyed the catalyst activity of **1a**/HBF₄·OEt₂ toward the hydrogenation of a number different alkenes (Table 2). In general, the rate of hydrogenation catalyzed by **1a**/HBF₄·OEt₂ was found to be ca. 2–3 times higher than the reactions catalyzed by **1a** alone. Furthermore, the increased activity was observed without significantly increasing the isomerization rate for terminal alkenes with β-hydrogens. More than a 4-fold rate increase has been observed for 5-hexen-2-one (entries 7, 8). The terminal alkene is preferentially hydrogenated over the internal one for the 4-vinyl-1-cyclohexene case (entries 9, 10). Since the major portion of isomerization products was found to be formed during the sample preparation period,¹¹ the formation of the isomerization products can be effectively suppressed by applying H₂ pressure to the solution containing the catalyst **1a** before adding alkene substrates.

Reaction of 1a with HBF₄·OEt₂. We thought that the increased catalyst activity of **1a**/HBF₄·OEt₂ might be due to the selective entrapment of the phosphine ligand and the formation of the 14-electron ruthenium–monophosphine species. The stoichiometric reactions of **1a** with different acids were examined to detect/isolate reactive intermediate species. Thus, the treatment of **1a** with 1.2 equiv of HBF₄·OEt₂ in C₆H₆ at room temperature led to the formation of the new complex **2** and Cy₃PH⁺BF₄⁻ in 1:3.5 ratio, as determined by ³¹P NMR (eq 2). The product mixture of **2**/Cy₃PH⁺BF₄⁻ was



isolated after simple precipitation/filtration procedures from the solution. Unfortunately, numerous attempts to separate **2** from the phosphonium salt thus far have not been successful because of the similar solubility property for both **2** and Cy₃PH⁺BF₄⁻ and due to the instability of **2** in solutions. The NMR spectroscopic data of **2**, the metal–hydride peak at δ -10.52 (d, *J*_{HP} = 25.2 Hz), and the carbonyl carbon peak at δ 196.9 (d, *J*_{CP} = 17.6 Hz) clearly indicated that the complex contains only one phosphine ligand per each ruthenium center. Furthermore, a relatively high CO stretching band (*ν*_{CO} = 1969 cm⁻¹) suggested a cationic nature of the complex. The greater amount of the phosphonium salt compared to **2** indicated that most of the Cy₃PH⁺BF₄⁻ resulted from the protonation of the second phosphine ligand.¹³ The isolated **2**/Cy₃PH⁺BF₄⁻ mixture was found to exhibit activity similar to the in-situ generated **1a**/HBF₄·OEt₂ under similar reaction conditions (TON = 2750 h⁻¹ for cyclooctene at 1.0 atm of H₂).

As mentioned, the C₆H₆ solution of the **2**/Cy₃PH⁺BF₄⁻ mixture was not stable at room temperature and slowly decomposed into a novel tetrameric ruthenium complex **3** along with other unidentified ruthenium products.¹⁴

(13) The IR spectra of isolated **2**/Cy₃PH⁺ showed little of other carbonyl-containing species, but we cannot rigorously rule out the presence of byproducts having no phosphine ligands. The elemental analyses on several samples of **2**/Cy₃PH⁺ gave disparate results.

(14) Complex **3** was isolated in 15–20% yields based on **1a**. Selected spectroscopic data of **3**: ³¹P{¹H} NMR (CD₂Cl₂, 121.6 MHz) δ 76.1 (s, PCy₃); IR (CH₂Cl₂) *ν*_{CO} = 1997 cm⁻¹.

(10) Yi, C. S.; Lee, D. W.; Chen, Y. *Organometallics* **1999**, *18*, 2043–2045.

(11) Yi, C. S.; Lee, D. W. *Organometallics* **1999**, *18*, 5152–5156.

(12) For the synthesis and reactions of **1b**, see: (a) Bull, M. L.; Elipse, S.; Esteruelas, M. A.; Oñate, E.; Peinado, E.; Ruiz, N. *Organometallics* **1997**, *16*, 5748–5755, and references therein. (b) Esteruelas, M. A.; Werner, H. J. *Organomet. Chem.* **1986**, *303*, 221–231. (c) Esteruelas, M. A.; Valero, C.; Oro, L. A.; Meyer, U.; Werner, H. *Inorg. Chem.* **1991**, *30*, 1159–1160. (d) Esteruelas, M. A.; Oro, L. A.; Valero, C. *Organometallics* **1992**, *11*, 3362–3369. (e) Esteruelas, M. A.; Herrero, J.; Oro, L. A. *Organometallics* **1993**, *12*, 2377–2379.

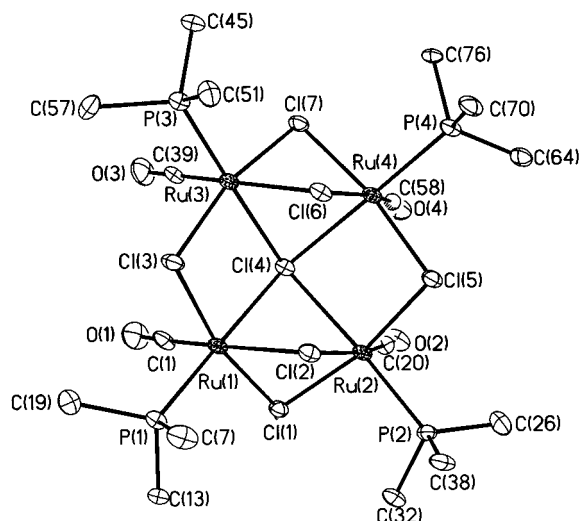
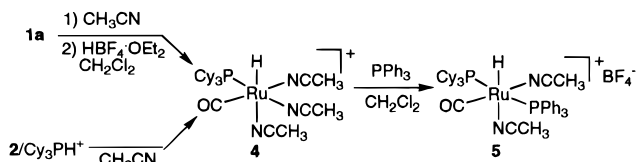


Figure 1. Molecular structure of **3** drawn with 30% thermal ellipsoids. Hydrogen atoms, BF_4^- ion, solvent molecules, and the carbon atoms of cyclohexyl group except ipso carbons are omitted for clarity.

Scheme 1



The single crystals of **3** grown from C_6H_6 solution were found to be suitable for X-ray crystallography (Figure 1). The molecular structure of **3** showed a tetrameric ruthenium center, in which two symmetric $[(\text{Cy}_3\text{P})(\text{CO})\text{-RuCl}]_2$ units are joined by three bridging chlorides and where all four CO ligands are in syn configuration with a overall pseudo C_{2v} symmetry. One of the most unusual structural features of **3** is the tetrabridging chloride ligand on the complex. While a few examples of tetrabridging chloride on late metal complexes of Cu, Cd, Ag, and Hg have been reported,¹⁵ to the best of our knowledge, this is a unique example of having a $\mu_4\text{-Cl}$ ligand for group VIII metal species. Hawthorne and Puddephatt independently observed the preferential μ_4 -coordination of the chloride ion by tetrameric Ag and Hg complexes.^{15a,b} One possible route to the formation of **3** is from the addition of Cl^- to an initially formed tetrameric unit of Ru_4^{2+} , in which the trapping of a Cl^- might have been driven by a highly electrophilic tetrameric Ru_4^{2+} metal center. It is also worthwhile to note that a tetrazirconium complex with a nonclassical, planar μ_4 -phosphonium ion has been recently reported.¹⁶

In an attempt to further establish the structure of **2**, we next explored the reaction of **1a** with acids in a

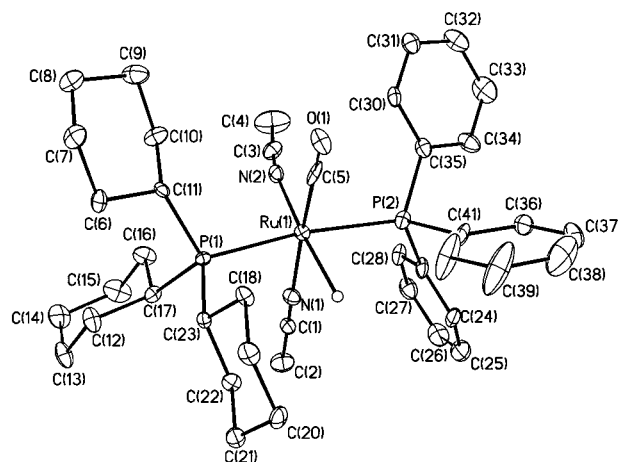


Figure 2. Molecular structure of the cation part of **5** drawn with 30% thermal ellipsoids. Hydrogen atoms except the metal-hydride, the solvent molecule, and the BF_4^- ion are omitted for clarity.

coordinating solvent. For example, when the reaction of **1a** (100 mg, 0.14 mmol) with $\text{HBF}_4\cdot\text{OEt}_2$ (25 μL , 1.2 equiv) was conducted in CH_3CN , the formation of a new monophosphine adduct **4** was initially observed by NMR (Scheme 1). The ratio between **4** and $\text{Cy}_3\text{PH}^+\text{BF}_4^-$ was found to be $\sim 1:1$, indicating that the selective entrapment of PCy_3 has been effected by the acid in this case. Due to the thermal instability of **4** in solution, its structure was tentatively established by spectroscopic methods at low temperature.¹⁷ The NMR data of **4**, which exhibited the ruthenium-hydride peak at $\delta -13.73$ (d, $J_{\text{PH}} = 22.2$ Hz) and the carbonyl peak at $\delta 202.3$ (d, $J_{\text{PC}} = 17.4$ Hz), clearly indicated that the complex contained only one phosphine ligand. Also, a relatively high CO stretching band ($\nu_{\text{CO}} = 1951\text{ cm}^{-1}$) is consistent with a cationic metal complex. Interestingly, dissolution of the isolated $2/\text{Cy}_3\text{PH}^+\text{BF}_4^-$ mixture in CH_3CN formed the same complex **4**, suggesting that a common 14-electron fragment is involved in both cases.

Further treatment of **4** with excess PPh_3 at room temperature produced the stable adduct **5** in 75% yield. One of the most diagnostic spectroscopic features of **5** was the AB pattern of two phosphorous peaks ($\delta 47.5$, $J_{\text{AB}} = 238$ Hz) resulting from their inequivalent environments. The metal-hydride peak at $\delta -13.57$ with a relatively small coupling constant (t, $J_{\text{PH}} = 18.0$ Hz) was consistent with the hydride ligand cis to both phosphine ligands. The structure of **5** was further established by X-ray crystallography (Figure 2). The molecular structure of **5** clearly showed an octahedral arrangement around the metal center with two trans phosphine ligands and two cis CH_3CN ligands.

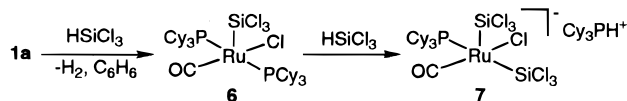
Reaction of 1a with a Weak Acid, HSiCl_3 . Since a relatively strong acidity of $\text{HBF}_4\cdot\text{OEt}_2$ might have caused the protonation of the second PCy_3 ligand, we explored the reaction of **1a** with weak acids in the hope of effecting a more selective entrapment of the single phosphine ligand. When the reaction of **1a** with the

(15) (a) Xu, W.; Vittal, J. J.; Puddephatt, R. J. *J. Am. Chem. Soc.* **1993**, *115*, 6456–6457. (b) Yang, X.; Knobler, C. B.; Zheng, Z.; Hawthorne, M. F. *J. Am. Chem. Soc.* **1994**, *116*, 7142–7159. (c) Oliver, K. J.; Waters, T. N.; Cook, D. F.; Rickard, C. E. F. *Inorg. Chim. Acta* **1977**, *24*, 85–89. (d) Wuest, J. D.; Zacharie, B. *Organometallics* **1985**, *4*, 410–411. (e) Beauchamp, A. L.; Oliver, M. J.; Wuest, J. D.; Zacharie, B. *J. Am. Chem. Soc.* **1986**, *108*, 73–77. (f) Yang, X.; Knobler, C. B.; Hawthorne, M. F. *Angew. Chem., Int. Ed. Engl.* **1991**, *30*, 1507–1508. (g) González-Durarte, P.; Clegg, W.; Casals, I.; Sola, J.; Rius, J. *J. Am. Chem. Soc.* **1998**, *120*, 1260–1266.

(16) (a) Driess, M.; Aust, J.; Mertz, K.; van Wüllen, C. *Angew. Chem., Int. Ed. Engl.* **1999**, *38*, 3677–3680. (b) Stephan, D. W. *Angew. Chem., Int. Ed. Engl.* **2000**, *39*, 501–502.

(17) Selected spectroscopic data of **4**: ^1H NMR (CD_2Cl_2 , 300 MHz, -45°C) $\delta -13.73$ (d, $J_{\text{PH}} = 22.2$ Hz, Ru–H), 2.05 (s, CH_3CN); $^{13}\text{C}\{^1\text{H}\}$ NMR (CD_2Cl_2 , 75.6 MHz, -30°C) $\delta 202.3$ (d, $J_{\text{PC}} = 17.4$ Hz, CO); $^{31}\text{P}\{^1\text{H}\}$ NMR (CD_2Cl_2 , 121.6 MHz, -30°C) $\delta 64.6$ (s, PCy_3); IR (CH_2Cl_2) $\nu_{\text{CO}} = 1951\text{ cm}^{-1}$.

Scheme 2



weak acid HSiCl_3 (2.2 equiv) in toluene- d_8 was monitored by NMR at room temperature, the formation of the new complex **6** was initially observed along with extensive H_2 gas evolution (Scheme 2). In the ^{31}P NMR spectra, the phosphorus signal of **6** (δ 36.9) initially appeared at the expense of **1a**, which gradually converted to an insoluble yellow-orange solid, **7**, within 30 min at room temperature. Due to the instability of the complex, we tentatively assigned the structure of **6** based on the available spectroscopic data. The ^{31}P NMR of the isolated **7** in CD_2Cl_2 exhibited two different phosphorus peaks, one assignable to the phosphonium ion (δ 28.4) and the other bonded to the ruthenium center, as indicated by the presence of ^{29}Si satellites (δ 30.1, $J_{\text{PSi}} = 51.3$ Hz).

The structure of **7** was further established by X-ray crystallography (Figure 3). The molecular structure of **7** showed that the complex still retained a square pyramidal geometry on the ruthenium center, with two silyl groups occupying each basal and apical positions. A considerably longer basal Ru–Si bond distance (2.316(2) Å) compared to the apical one (2.249(2) Å) indicated a strong trans influence from the phosphine ligand to the basal silyl group. In this case, a selective transformation of the phosphine ligand into the phosphonium ion has been achieved with 2 equiv of HSiCl_3 . The initial H_2 gas formation suggested that the protonation at the metal was preferred over the direct protonation at the phosphine ligand.

Deuterium-Labeling Studies and the Formation of the $\eta^2\text{-H}_2$ Complex. In an attempt to elucidate the source of the metal–hydride of **2**, the reaction of the deuterated **1a-d**₁ (>95% D) with 4 equiv of $\text{HBF}_4\cdot\text{OEt}_2$ in CD_2Cl_2 was monitored by NMR at room temperature (Scheme 3).¹⁸ Initially formed **2** contained ~10% deuterium on the metal–hydride, while the phosphonium salt had a ~4:1 ratio of $\text{Cy}_3\text{PH}^+\text{BF}_4^-$ to $\text{Cy}_3\text{PD}^+\text{BF}_4^-$. When the reaction of **1a-d**₁ with $\text{HBF}_4\cdot\text{OEt}_2$ was conducted in CD_3CN , reappearance of the ruthenium–hydride peak of **1a** was initially observed by ^1H NMR at room temperature. Again, a 4:1 ratio of Cy_3PH^+ to Cy_3PD^+ was observed for the phosphonium salt.¹⁹ The H/D ratio of the phosphonium salt was found to depend on the amount of acid; for example, addition of 10 equiv of $\text{HBF}_4\cdot\text{OEt}_2$ led to a ~10:1 ratio of Cy_3PH^+ to Cy_3PD^+ . The deuterium content of **4** could not be accurately estimated in this case, since the complex **4** rapidly decomposed in solution, which prevented obtaining a meaningful ^2H NMR.

The evolution of H_2 gas during the reaction of **1a** with HSiCl_3 and the rapid H/D exchange implied the formation of a $\eta^2\text{-H}_2$ intermediate species. In an effort to detect the $\eta^2\text{-H}_2$ complex, the reaction of **1a** with $\text{HBF}_4\cdot\text{OEt}_2$

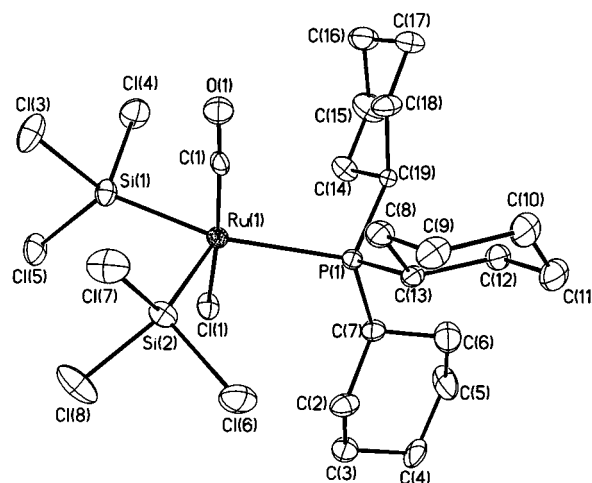


Figure 3. Molecular structure of the anion part of **7** drawn with 30% thermal ellipsoids. Hydrogen atoms and the phosphonium ion are omitted for clarity.

in 1:1 toluene- d_8 / CD_3CN was monitored by ^1H NMR at low temperature. At -45°C , the new broad metal–hydride peak appeared at $\delta -9.80$, which was consistent with the formation of the $\eta^2\text{-H}_2$ complex **8**. The hydride signal of **8** was gradually disappeared within 30 min at -45°C as the peaks due to **4** began to appear. The formation of the $\eta^2\text{-H}_2$ complex was further established from the reaction of deuterated **1a-d**₁ with $\text{HBF}_4\cdot\text{OEt}_2$. In this case, the hydride peak turned into a characteristic 1:1:1 triplet ($J_{\text{HD}} = 29.3$ Hz), which is consistent with the formation of the $\eta^2\text{-HD}$ complex **8-d**₁ (Figure 4). Though not completely resolved, each 1:1:1 triplet peak appeared to be further split into small triplets ($J_{\text{HP}} < 7$ Hz) due the coupling with two phosphorus atoms.²⁰ Previously, numerous stable $\eta^2\text{-H}_2$ complexes of ruthenium and osmium complexes have been reported.²¹

The spectroscopic observation of the $\eta^2\text{-H}_2$ complex **8** in the reaction with **1a-d**₁ is consistent with the rapid protonation at the metal center prior to the elimination of Cy_3PH^+ . The apparent statistical distribution of the deuterium atom (approximately 20% deuterium incorporation into the phosphonium salt with 4 equiv of the acid) also suggests that the initial H/D exchange via the formation of the $\eta^2\text{-H}_2$ complex **8** is much faster than the subsequent elimination of Cy_3PH^+ salt. The addition of excess PPh_3 to the solution containing **4** led to **5** with the same amount of deuterium (20%), indicating that no further H/D exchange had occurred during the formation of **5**. As evidenced by the formation of the cationic complex **5**, the Cl^- ligand dissociation became a competitive process especially in the coordinating solvent CH_3CN .

(20) Several attempts for T_1 measurement of **8** were not successful because of a relatively short lifetime of the complex at low temperature.

(21) (a) Chinn, M. S.; Heinekey, D. M. *J. Am. Chem. Soc.* **1990**, *112*, 5166–5175. (b) Gusev, D. G.; Vymenits, A. B.; Bakhmutov, V. I. *Inorg. Chem.* **1992**, *31*, 2–4. (c) Esteruelas, M. A.; Lahoz, F. J.; Oñate, E.; Oro, L. A.; Valero, C.; Zeier, B. *J. Am. Chem. Soc.* **1995**, *117*, 7935–7942. (d) Bakhmutov, V. I.; Bertrán, J.; Esteruelas, M. A.; Lledós, A.; Maseras, F.; Modrego, J.; Oro, L. A.; Sola, E. *Chem. Eur. J.* **1996**, *2*, 815–825. (e) Gusev, D. G.; Kuhlman, R. L.; Renkema, K. B.; Eisenstein, O.; Caulton, K. G. *Inorg. Chem.* **1996**, *35*, 6775–6783. (f) Luther, T. A.; Heinekey, D. M. *Inorg. Chem.* **1998**, *37*, 127–132. (g) Gründemann, S.; Ulrich, S.; Limbach, H.-H.; Golubev, N. S.; Denisov, G. S.; Epstein, L. M.; Sabo-Étienne, S.; Chaudret, B. *Inorg. Chem.* **1999**, *38*, 2550–2551.

(18) Approximately 4 equiv of the acid was required to complete the reaction.

(19) The H/D ratio of the phosphonium salt was determined by ^{31}P NMR. The phosphorous signal of Cy_3PD^+ at δ 29.3 (1:1:1 triplet, $J_{\text{PD}} = 71$ Hz) was approximately 1 ppm upfield-shifted compared to the signal of Cy_3PH^+ (δ 30.2).

Scheme 3

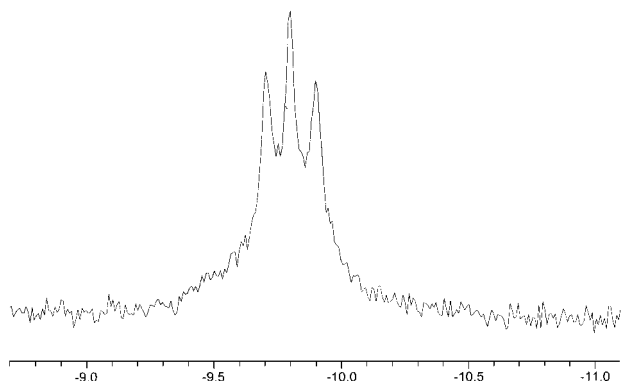
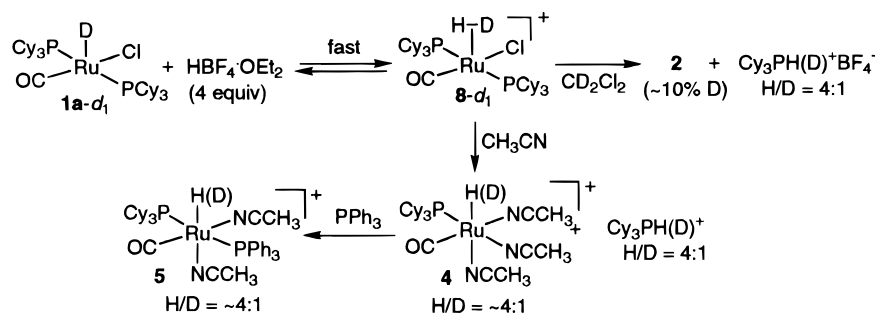
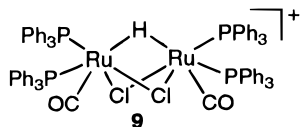


Figure 4. ^1H NMR of the metal–hydride region of **8-d₁** in toluene- d_8 /CD $_3$ CN (1:1) at $-45\text{ }^\circ\text{C}$.

These results implicate the involvement of a 14-electron species as the key intermediate in the catalytic hydrogenation reaction. The substantial rate increase in the reactions catalyzed by **1a**/HBF $_4$ ·OEt $_2$ can be rationalized via the formation of a transient species, [(Cy $_3$ P)(CO)RuHCl], generated from the selective entrapment of the phosphine ligand. The selective formation of **4** and **7** from the reactions of **1a** with HBF $_4$ ·OEt $_2$ in CH $_3$ CN and with the weak acid HSiCl $_3$ also supports the formation of a monophosphine species. Caulton and co-workers recently reported the synthesis of stable cationic 14-electron ruthenium complexes, [(PBu $_2$ Me) $_2$ (CO)RuX] $^+$ Bar $_4$ $^-$ (X = H, CH $_3$, Ph, BC $_6$ H $_4$ O $_2$).²² These ruthenium complexes were shown to have a nonplanar “sawhorse” geometry, with M–H–C agostic interactions from the *t*-Bu groups of the two phosphine ligands. Baratta and co-workers reported a neutral 14-electron ruthenium complex, [PPh $_2$ (2,6-Me $_2$ C $_6$ H $_5$) $_2$ RuCl $_2$], which was also shown to be stabilized by having agostic interactions with the phosphine ligand.²³



Preliminary investigations indicated that the acid-induced selective entrapment of the phosphine ligand

is most effective for complexes with a sterically demanding PCy $_3$ ligand. It is interesting to note that analogous reaction of **1b** with HBF $_4$ ·OEt $_2$ did not give clean products; several unidentified phosphorus peaks appeared along with a significant amount of decomposition, as judged by the ^{31}P NMR. It was previously reported that the analogous reaction of (PPh $_3$) $_3$ (CO)(Cl)-RuH with aqueous HBF $_4$ formed the cationic complex [(PPh $_3$) $_2$ (CO)Ru(μ -Cl)] $_2$ (μ -H) $^+$ (**9**) with a bridging metal–hydride,²⁴ but the complex **9** was found to be completely inactive toward the hydrogenation reaction. Several similar dimeric structures with terminal metal–hydrides, which are consistent with the spectroscopic data of **2**, are currently being considered as a possible structure.

Conclusions

In summary, an acid-induced selective entrapment of the phosphine ligand from **1a** was found to give a substantial rate increase toward the hydrogenation of alkenes. The stoichiometric reaction of **1a** with HBF $_4$ ·OEt $_2$ led to the isolation of the mixture of **2** and Cy $_3$ PH $^+$ BF $_4^-$. The selective entrapment of the phosphine ligand has been demonstrated in the stoichiometric reactions of **1a** with HBF $_4$ ·OEt $_2$ in CH $_3$ CN and with the weak acid HSiCl $_3$. These results together with the observation of the η^2 -H $_2$ complex **8** suggested the involvement of the monomeric 14-electron species in the catalytic reaction. Further structure elucidation and the exploration of the catalyst activity of **2** toward other reactions are currently being pursued.

Experimental Section

General Information. All reactions were carried out in an inert-atmosphere glovebox or by using standard high-vacuum and Schlenk line techniques unless otherwise noted. Benzene, hexanes, and Et $_2$ O were distilled from purple solutions of sodium and benzophenone immediately prior to use. CH $_2$ Cl $_2$ was distilled from CaH $_2$. The NMR solvents were dried from activated molecular sieves (4 Å). All organic alkene substrates were purchased from commercial sources and vacuum-distilled from either molecular sieves or sodium prior to use. The acids, HBF $_4$ ·OEt $_2$ and HSiCl $_3$, were purchased from Aldrich Chemical Co. and used without further purification. The complexes **1a** and **1b** were prepared according to the previously reported procedure.^{10,12} The ^1H , ^{13}C , and ^{31}P NMR spectra were recorded on a GE GN-Omega 300 MHz FT-NMR spectrometer. Infrared and mass spectra were recorded from Nicolet Magna 560 and Hewlett-Packard HP 5890 GC/MS

(22) (a) Huang, D.; Huffman, J. C.; Bollinger, J. C.; Eisenstein, O.; Caulton, K. G. *J. Am. Chem. Soc.* **1997**, *119*, 7398–7399. (b) Huang, D.; Oliván, M.; Huffman, J. C.; Eisenstein, O.; Caulton, K. G. *Organometallics* **1998**, *17*, 4700–4706. (c) Huang, D.; Streib, W. E.; Bollinger, J. C.; Caulton, K. G.; Winter, R. F.; Scheiring, T. *J. Am. Chem. Soc.* **1999**, *121*, 8087–8097.

(23) Baratta, W.; Herdtweck, E.; Rigo, P. *Angew. Chem., Int. Ed. Engl.* **1999**, *38*, 1629–1631.

(24) Sánchez-Delgado, R. A.; Thewalt, U.; Valencia, N.; Andriollo, A.; Márquez-Silva, R.-L.; Puga, J.; Schöllhorn, H.; Klein, H.-P.; Fontal, B. *Inorg. Chem.* **1986**, *25*, 1097–1106.

Table 2. Hydrogenation of Alkenes Catalyzed by 1/HBF₄·OEt₂^a

entry	alkene	catalyst	additive	H ₂ (atm)	turnover rate ^b
1	1-hexene	1a	none	1.0	1200 (180)
2		1a	HBF ₄ ·OEt ₂	1.0	2250 (500)
3	1-hexene	1b	none	1.0	700 (200)
4		1b	HBF ₄ ·OEt ₂	1.0	800 (200)
5	allylbenzene	1a	none	2.0	2000 (390)
6		1a	HBF ₄ ·OEt ₂	2.0	3000 (240)
7	5-hexen-2-one	1a	none	2.0	240 (24)
8		1a	HBF ₄ ·OEt ₂	2.0	1100 (60)
9	4-vinyl-1-cyclohexene	1a	none	2.0	1300
10		1a	HBF ₄ ·OEt ₂	2.0	3100

^a Reaction conditions: 5.7 mmol of alkene (1.0 M); 0.69 μmol of the catalyst (0.12 mM; alkene:**1a** = 8300:1); 1–2 equiv of the acid; 5 mL of C₆H₆; 22 ± 1 °C. ^b Turnover rate = (mol of product)/(mol of catalyst) h⁻¹; the numbers in parentheses correspond to the isomerization rate.

Table 3. Crystallographic Data for [Ru₄(Cl)₇(PCy₃)₄(CO)₄]⁺BF₄⁻ (3**), [(PCy₃)(PPh₃)(CH₃CN)₂(CO)RuH]⁺BF₄⁻ (**5**), and Cy₃PH⁺[(PCy₃)(CO)(SiCl₃)₂RuCl]⁻ (**7**)**

	C ₈₈ H ₁₄₄ BCl ₇ F ₄ O ₄ P ₄ Ru ₄ (3)	C _{43.5} H _{58.5} BCl ₂ F ₄ N ₂ OP ₂ Ru (5)	C ₃₇ H ₆₇ Cl ₇ OP ₂ RuSi ₂ (7)
formula wt	2129.15	946.14	995.25
space group	<i>P</i> $\bar{1}$	<i>P</i> $\bar{1}$	<i>P</i> $\bar{1}$
<i>a</i> , Å	14.9933(2)	10.288(2)	11.7530(2)
<i>b</i> , Å	17.6503(2)	17.352(4)	20.0661(2)
<i>c</i> , Å	21.6833(2)	26.729(5)	21.2648(3)
α , deg	84.3204(5)	76.517(5)	110.1073(9)
β , deg	84.7235(5)	82.826(4)	92.4954(8)
γ , deg	72.5387(2)	79.354(4)	91.5251(5)
<i>V</i> , Å ³	5418.13(9)	4543(3)	4700.30(13)
<i>Z</i> , <i>Z'</i>	2, 1	4	4, 2
cryst color, habit	red brick	colorless block	orange block
<i>D</i> (calc), g cm ⁻³	1.301	1.383	1.406
μ (Mo K α), cm ⁻¹	8.24	5.84	8.79
temp, K	220(2)	173(2)	173(2)
diffractometer		Siemens P4/CCD	
radiation		Mo K α (λ = 0.71073 Å)	
<i>R</i> (<i>F</i>), % ^a	9.90	8.94	4.70
<i>R</i> (<i>wF</i> ²), % ^a	20.19	19.01	16.07

^a Quantity minimized = $R(wF^2) = \sum [w(F_o^2 - F_c^2)] / \sum [(wF_o^2)^{1/2}]$; $R = \sum \Delta / \sum (F_o)$, $\Delta = |F_o - F_c|$, $w = 1/[\sigma^2(F_o^2) + (aP)^2 + bP]$, $P = [2F_c^2 + \max(F_o, 0)]/3$.

spectrometers, respectively. Gas chromatographs were recorded from a Hewlett-Packard HP 6890 GC spectrometer.

General Procedure of the Catalytic Hydrogenation Reaction. In a glovebox, 1.0 mL of a predissolved 0.69 mM C₆H₆ solution of complex **1a** (0.5 mg, 0.69 μmol) and HBF₄·OEt₂ (0.1 μL, 1.0 equiv) was placed in a 100 mL Schlenk flask equipped with a stirring bar. The solution was diluted with 4.0 mL of C₆H₆. Excess alkene (5.7 mmol) was added, and the bottle was attached to a vacuum line. The reaction bottle was evacuated while it was cooled in a liquid N₂ bath. The 1.0 atm of H₂ gas was applied to the reaction bottle, and the reaction mixture was vigorously stirred at room temperature (22–23 °C) for 0.5–2 h. For reactions at higher pressure of H₂, a Fisher-Porter pressure bottle was used. The product yield was determined by GC.

Preparation of **2.** To a C₆H₆ (5 mL) suspension of complex **1a** (100 mg, 0.14 mmol) was added HBF₄·OEt₂ (54 wt %, 25 μL, 1.2 equiv) via syringe in three portions at 1 h intervals at room temperature. After the solution was concentrated to 1 mL, it was triturated with 10 mL of hexanes. The resulting brick-colored precipitate was washed three times with hexanes. The product mixture of **2** and Cy₃PH⁺BF₄⁻ (1:3.5) was isolated after the removal of solvents under vacuum (yield of **2** = ~15%).

Spectroscopic data of **2**: ¹H NMR (CD₂Cl₂, 300 MHz) δ -10.52 (d, *J*_{PH} = 25.2 Hz, Ru–H); ¹³C{¹H} NMR (CD₂Cl₂, 75.6 MHz) δ 196.9 (d, *J*_{PC} = 17.6 Hz, CO); ³¹P{¹H} NMR (CD₂Cl₂, 121.6 MHz) δ 73.8 (s, PCy₃); IR (CH₂Cl₂) ν _{CO} = 1969 cm⁻¹.

Preparation of [(PCy₃)(PPh₃)(CH₃CN)₂(CO)RuH]⁺BF₄⁻ (5**).** To a suspension of **1a** (100 mg, 0.14 mmol) in CH₂Cl₂ solution was added 0.1 g of CH₃CN (2.3 mmol) via a syringe at room temperature. The reaction mixture turned into a pale

yellow homogeneous solution within 1 min. The acid HBF₄·OEt₂ (54 wt %, 25 μL, 1.2 equiv) was added via a syringe into the solution, and the solution was stirred for 5 min. The ³¹P NMR of the solution showed the clean formation of **4** at this time. Excess PPh₃ (45 mg, 0.17 mmol) was added to this solution at room temperature, and the reaction mixture was stirred for 10 min. Solvent was removed under vacuum, and the residue was filtered through a short silica column using CH₃CN as an eluent. The filtrate was concentrated to ~1 mL and was precipitated by adding ~10 mL of hexanes. The resulting solid was filtered and washed with hexanes (3 × 5 mL). Drying under vacuum gave the product **5** as an off-white solid (75%).

For **5:** ¹H NMR (CD₂Cl₂, 300 MHz) δ -13.57 (pseudo t, *J*_{PH} = 18.0 Hz, Ru–H), 7.9–7.4 (m, PPh₃), 2.2–1.2 (m, PCy₃), 1.95 (s, CH₃CN); ¹³C{¹H} NMR (CD₂Cl₂, 75.6 MHz) δ 203.4 (pseudo t, *J*_{CP} = 13.9 Hz, CO), 125.1 (s, CH₃CN), 3.2 (pseudo q, *J* = 4.0 Hz, CH₃CN); ³¹P{¹H} NMR (CD₂Cl₂, 121.6 MHz) δ 47.5 (AB quartet, *J*_{AB} = 236 Hz, PPh₃ and PCy₃); IR (CH₂Cl₂) ν _{CO} = 1952 cm⁻¹; FAB-MS 669.2 (M⁺ – (H + 2 CH₃CN)).

Preparation of Cy₃PH⁺[(PCy₃)(CO)(SiCl₃)₂RuCl]⁻ (7**).** To a C₆H₆ (20 mL) suspension of **1a** (300 mg, 0.41 mmol) was added HSiCl₃ (100 μL, 1.0 mmol, 2.4 equiv) dropwise via a syringe at room temperature. The reaction mixture was stirred for 2 h at room temperature. The resulting pale yellow solution was concentrated to ~5 mL and was precipitated by adding hexanes (10 mL). The resulting solid was filtered through a frit and washed with hexanes (3 × 10 mL). After drying under vacuum, the product **7** was isolated in 85% yield as a pale yellow solid.

For **7:** ¹H NMR (CD₂Cl₂, 300 MHz) δ 6.03 (dq, *J*_{PH} = 462 Hz, *J*_{HH} = 0.9 Hz, HPCy₃); ¹³C{¹H} NMR (CD₂Cl₂, 75.6 MHz)

δ 198.9 (d, $J_{\text{PC}} = 8.4$ Hz, CO); $^{31}\text{P}\{^1\text{H}\}$ NMR (CD_2Cl_2 , 121.6 MHz) δ 30.1 (s, $J_{\text{PSi}} = 51.3$ Hz, PCy_3), 28.4 (s, HPCy_3^+); IR (CH_2Cl_2) $\nu_{\text{CO}} = 1946$ cm^{-1} .

NMR Reaction of 1a with $\text{HBF}_4 \cdot \text{OEt}_2$. In a NMR tube capped with rubber septum, complex **1a** (6 mg, 8.3 μmol) was dissolved in a 1:1 mixture of toluene- d_8 / CD_3CN at room temperature, and the tube was cooled in a dry ice/acetone bath. The acid $\text{HBF}_4 \cdot \text{OEt}_2$ (54 wt %, 4.8 μL , 4 equiv) was carefully added to the top of the solution via a syringe. The tube was shaken several times while it was immersed in a dry ice/acetone bath. The tube was inserted into a precooled NMR probe at -50 $^\circ\text{C}$.

Selected spectroscopic data of **8**: ^1H NMR (1:1 toluene- d_8 / CD_3CN , 300 MHz, -45 $^\circ\text{C}$) δ -9.80 (br s); $^{31}\text{P}\{^1\text{H}\}$ NMR (1:1 toluene- d_8 / CD_3CN , 121.6 MHz, -45 $^\circ\text{C}$) δ 35.3 (s, PCy_3).

Crystallographic Structural Determination. Single crystals of **3**, **5**, and **7** suitable for X-ray crystallographic analysis were grown from benzene/hexanes and CH_2Cl_2 /hexanes solutions, respectively. The data collections were performed on a Siemens P4/CCD diffractometer. The crystallographic data for complexes **3**, **5**, and **7** are summarized in Table 3. Systematic absences and diffraction symmetry were uniquely consistent for the reported space groups, whose correctness was subsequently confirmed by chemically reasonable and computationally stable results of refinement. The structures were solved by using direct methods, completed by subsequent difference Fourier synthesis and refined with full-matrix, least-squares procedures. The DIFABS empirical absorption corrections were applied to the data sets of **3**, while

the SADABS were applied to both **5** and **7**. One full molecule of benzene and two-half molecules of benzene were present in a unit cell of **3**. The BF_4^- anion was positionally disordered in a 61:39 distribution about F(1). The asymmetric unit of **5** contained two cationic ruthenium complexes, two BF_4^- ions, and a half benzene molecule. The BF_4^- anion and one of the Cy groups were positionally disordered. The asymmetric unit of **7** contained two ruthenium anion and two Cy_3PH^+ cation parts and was disordered over two positions with a 80:20 distribution. All non-hydrogen atoms were refined with anisotropic displacement coefficients except B(1') and C(58) of **3**. All hydrogen atoms were treated as idealized contributions, except for the hydrogen atoms of the disordered Cy group of **5** and the Cy_3PH^+ cation of **7**, which were not located. All software and sources of the scattering factors are contained in the SHELXTL (version 5.10) program library (G. Sheldrick, Siemens XRD, Madison, WI).

Acknowledgment. Financial support from the National Institutes of Health (R15 GM55987) and the donors of the Petroleum Research Fund, administered by the American Chemical Society, is gratefully acknowledged.

Supporting Information Available: X-ray crystallographic data of **3**, **5**, and **7** (PDF). This material is available free of charge via the Internet at <http://pubs.acs.org>.

OM000315N